Molecular Dynamics Study on the Adsorption Selectivity for Negative Elements in Aluminosilicates

Masahiko Matsumiya and Ryuzo Takagi[a]

Matsumiya Computational Chemistry Institute,
6-14 higashi-numa, machiya-aza, chiaki-cho, ichinomiya-shi, Aichi 491-0813 Japan
[a] Research Laboratory for Nuclear Reactors, Tokyo Institute of Technology,
O-okayama, Meguro-ku, Tokyo 152-8550 Japan

Reprint requests to Prof. M. M.; Fax: 81 586-76-6473; E-mail: molten@d9.dion.ne.jp

For the pyrochemical reprocessing of spent metallic nuclear fuels in molten salt baths it is important to investigate the adsorption selectivity of cations in aluminosilicates. A molecular dynamics simulation has been performed on sodalite and zeolite with exchangeable monovalent and multivalent cationic fission products at 673 K in order to calculate their self-diffusion coefficients in the aluminosilicate framework and estimate the selectivity of the exchangeable cations. The results enables us to conclude that the self-diffusion coefficients of monovalent cations decrease with increasing ionic radius. The order of the adsorption selectivity is Li < K < Na < Cs in sodalite and Li < Na < K < Cs in zeolite. The self-diffusion coefficients of multivalent cations are almost independent of the ionic radius, and these cations are in aluminosilicates more stable than monovalent cations. The results are consistent with the experimental results.

Key words: Adsorption Selectivity; Aluminosilicates Framework; Molecular Dynamics Simulation; Negative Elements; Self-diffusion Coefficient; Sodalite; Zeolite.

1. Introduction

One should become able to separate fission products (FPs) like Cs and Sr from one another for incineration, utilization as medical tracers, precious materials, and so on. For this purpose we have developed pyrochemical processes [1] such as countercurrent electromigration [2] and electrowinning [3 - 7], as was proposed by the Argonne National Laboratory [8]. In addition, we have estimated the enrichment degree and investigated the electrochemical behavior of Cs in molten alkali ternary chloride [9 - 11] and fluoride [11] systems by both experiment and Molecular Dynamics (MD) simulation. These results lead to the conclusion that it is rather difficult to enrich and recover Cs in these systems, although we demonstrated that one can recover La^{3+} [12], Nd^{3+} [13], and Dy^{3+} [14, 15]. There are other candidates for processes to function as inorganic ion exchangers [16 - 18]. For example, aluminosilicates, e. g., sodalite and zeolite with their relatively rigid anionic framework which contains exchangeable cations and removable and replaceable guest molecules, are used commercially as catalysts, molecular sieves, absorbents, and selective ion exchangers. Some zeolites can absorb alkali and alkaline-earth cations according to their ionic radii in holes of different size. This technique could also be applied for the treatment of molten salts containing nuclear fission products [19].

Most simulation work on zeolite systems has been studied by MD methods. For example, Demontis and co-workers reported the positions and vibrations of water molecules in the cages of natrolite [20, 21], the atomic coordinates and the crystal symmetry of dehydrated natrolite [22] and Linde zeolite 4A [23], the diffusive motion of methane in silicate [24] and the structural changes of silicate at different temperatures [25]. Cohen de Lara and co-workers also performed an MD study of methane adsorbed in zeolite-A [26] based on their potential-energy calculation [27]. The dynamics of Na^+ ions inside a zeolite-A framework at several temperatures was described by a MD simulation by Shin et al. [28]. The purpose of the present work is to illuminate the selectivity of cations in the aluminosilicates framework through MD simulations at 673 K.

Table 1.1. The parameters used in the calculation for the sodalite framework and for the exchangeable cations.

Ion	Number	z/e	$a/Å$	$b/Å$	$c/\mathrm{kJ}^{1/2}Å^3\mathrm{mol}^{-1/2}$
Sodalite framework, $Na_6Al_6Si_6O_{24} \cdot 2\,NaCl$:					
Na	160	1.0	1.260	0.080	10.000
Al	120	3.0	1.064	0.080	0.000
Si	120	4.0	1.012	0.080	0.000
O	480	−2.0	1.629	0.085	20.000
Cl	40	−1.0	1.950	0.090	30.000
Exchangeable cations:					
Li	160	1.0	0.796	0.080	0.000
K	160	1.0	1.595	0.080	15.000
Cs	160	1.0	1.852	0.080	25.000
Sr	160	2.0	1.632	0.080	15.000
Ba	160	2.0	1.820	0.080	20.000
La	160	3.0	1.111	0.080	25.000
Nd	160	3.0	1.059	0.080	25.000

Table 1.2. The parameters used in the calculation for the zeolite framework and for the exchangeable cations.

Ion	Number	z/e	$a/Å$	$b/Å$	$c/\mathrm{kJ}^{1/2}Å^3\mathrm{mol}^{-1/2}$	Ion pair	$D/10^{-19}$	β	$r^*/Å$
Zeolite framework, $Na_{12}Al_{12}Si_{12}O_{48}$:									
Na	120	1.0	1.388	0.120	10.000	Al-O:	44.0	2.0	1.710
Al	120	2.25	1.022	0.080	0.000	Si-O:	74.0	2.0	1.510
Si	120	2.4	0.942	0.090	0.000				
O	480	−1.4125	1.908	0.150	29.200				
Exchangeable cations:									
Li	160	1.0	0.796	0.080	0.000				
K	160	1.0	1.595	0.080	15.000				
Cs	160	1.0	1.852	0.080	25.000				
Sr	160	2.0	1.632	0.080	15.000				
Ba	160	2.0	1.820	0.080	20.000				
La	160	3.0	1.111	0.080	25.000				
Nd	160	3.0	1.059	0.080	25.000				

2. The Molecular Dynamics Simulation

(a) Sodalite, $Na_6Al_6Si_6O_{24} \cdot 2\,NaCl$, P43n

920 particles were disposed in a periodic cube whose edge length L was determined from the density. The framework was assumed to be rigid and the following pair potentials were used with the initial position data of [29]:

$$\Phi_{ij} = \frac{z_i z_j e^2}{4\pi\varepsilon_0 r_{ij}} + f_0(b_i + b_j)\exp\left(\frac{a_i + a_j - r_{ij}}{b_i + b_j}\right) \quad (1)$$
$$- \frac{c_i c_j}{r^6},$$

where z is the positive or negative charge number, e the elementary charge and ε_0 the permittivity of vacuum. The first term in (1) represents the Coulomb interaction, the second the exponential repulsion and the third the dipole-dipole dispersion energy. Some data of the adopted values of z, a, b and c are listed in Table 1.1. Rigid framework simulations were carried out by Leherte et al. [30 - 33]. The Ewald method [34] was used for the calculation of the Coulomb forces; the cutoff distance in real space was $L/2$, and the reciprocal lattice vectors $|n^2|$ were counted up to 27. The convergence parameter a was $5.6/L$ and the time step 2fs. At the beginning, MD runs were performed with the constant temperature method proposed by Woodcock [35]. After constant temperature (673 K) runs of several thousand steps, these were switched to constant energy runs. From the runs during more

than 10^4 time steps, using Verlet's Algorithm after attainment of equilibrium, the self-diffusion coefficients and the adsorption selectivity were estimated.

(b) Zeolite, $Na_{12}Al_{12}Si_{12}O_{48}$, Pm3m

The zeolite framework is modeled by the pseudo cell, $(SiAlO_4)_{12}$, or the Pm3m space group which contains $12Na^+$ ions. The framework atoms are fixed in space at the positions determined by the X-ray diffraction experiment of Pluth and Smith [36] for the dehydrated zeolite. For the MD simulation, 840 particles were employed with the initial position data. The interatomic potential functions consist of Colombic, short range repulsion, van der Waals attraction, and Morse potential terms applied only to the interactions among aluminum, silicon and oxygen. Because of the small charge of Al and Si in the zeolite framework estimated from a quantum chemical study [37], the applied MD of zeolite is following a partially ionic potential model:

$$\Phi_{ij} = \frac{z_i z_j e^2}{4\pi\varepsilon_0 r_{ij}} + f_0(b_i + b_j)\exp\left(\frac{a_i + a_j - r_{ij}}{b_i + b_j}\right) \quad (2)$$
$$- \frac{c_i c_j}{r^6} + D_{ij}\left(\exp\left(2\beta_{ij}(r_{ij} - r^*_{ij})\right)\right.$$
$$\left. - 2\exp\left(\beta_{ij}(r_{ij} - r^*_{ij})\right)\right),$$

where r_{ij} is an interatomic distance and f_0 is a constant. The parameters, z, a, b and c, are for the atomic
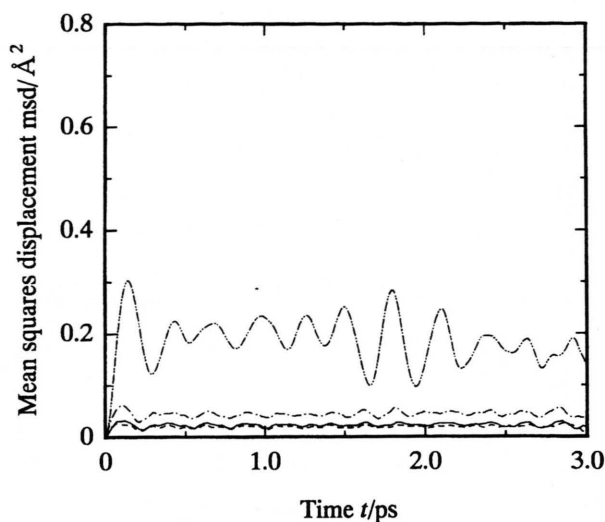
Fig. 1. Relationship between the mean squares displacements of sodalite framework and the time at 673 K. Al: solid line, Si: broken line, O: chain line, Cl: double chain line.

Table 2.1. Self-diffusion coefficients, calculated from the mean squares displacement in the sodalite framework and exchangeable cations.

Ion	Ionic radius/pm	$D/10^{-6}(cm^2/s)$
Sodalite framework:		
Na	117.0	2.17
Al	—	0.39
Si	—	0.33
O	—	0.74
Cl	158.5	3.12
Exchangeable cations:		
Li	81.6	7.57
K	146.3	3.07
Cs	172.0	1.68
Sr	118.0	2.86
Ba	135.0	1.08
La	103.2	0.88
Nd	98.3	1.24

Table 2.2. Self-diffusion coefficients, calculated from the mean squares displacement in the zeolite framework and exchangeable cations.

Ion	Ionic radius/pm	$D/10^{-6}(cm^2/s)$
Sodalite framework:		
Na	117.0	6.21
Al	—	0.39
Si	—	0.33
O	—	0.74
Exchangeable cations:		
Li	81.6	9.03
K	146.3	2.57
Cs	172.0	1.42
Sr	118.0	0.92
Ba	135.0	1.08
La	103.2	1.57
Nd	98.3	1.00

species, and D_{ij}, β_{ij} and r_{ij}^* are for the Al-O and Si-O pairs. All the parameters employed for zeolite are tabulated in Table 1.2. The calculation methods of the zeolite and sodalite systems, such as the algorithm are similar.

3. Results and Discussion

(a) Sodalite

The mean squares displacements (MSD) of the ions of the sodalite framework with time are shown in Figure 1. It is seen that the Cl⁻ ions are highly mobile and exchangeable. The MSD's of monovalent and multivalent cations are shown in Figure 2. The self-diffusion coefficients of the exchangeable cations within the sodalite system were calculated from the MSD's according to the Einstein equation [38] as summarized in Table 2.1 together with the ionic radius. The results obtained by the simulation predict that in the sodalite the order of the self-diffusion coefficients and the estimated adsorption selectivity for each cation would be

$$D_{Cs} < D_{Na} < D_K < D_{Li} \qquad (3a)$$
$$\text{(monovalent cations in sodalite)}$$

$$D_{La} \approx D_{Ba} \approx D_{Nd} < D_{Sr} \qquad (3b)$$
$$\text{(multivalent cations in sodalite)}$$

$$\text{Li} < \text{K} < \text{Sr} < \text{Na} < \text{Cs} < \text{Nd} < \text{Ba} < \text{La} \qquad (3c)$$
$$\text{(adsorption selectivity in sodalite)}$$

The self-diffusion coefficients of multivalent cations are smaller than that of the K ion. This means the multivalent ions, Na and Cs are more stable in sodalite than K and Li.

The velocity autocorrelation functions (VCF) for monovalent and multivalent exchangeable cations are shown in Figure 3. The VCF's oscillate continuously, decay rapidly to zero and have different depth and position of the first peak. The behavior of the MSD's is common: a short, rapid increase and then slow, flat changes, which also indicates random moving in closed cages, but of different sizes.
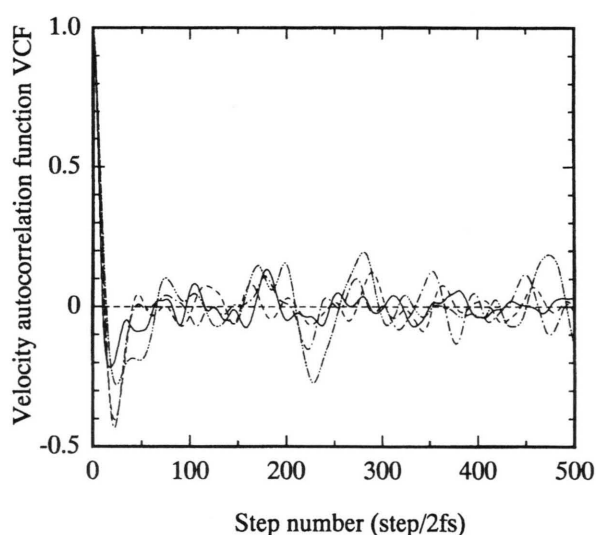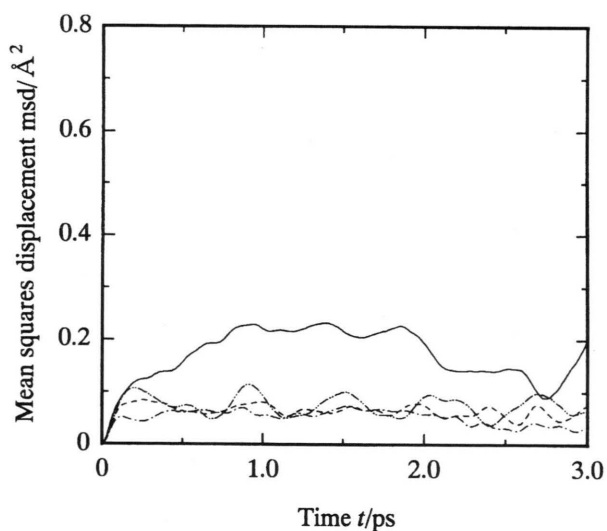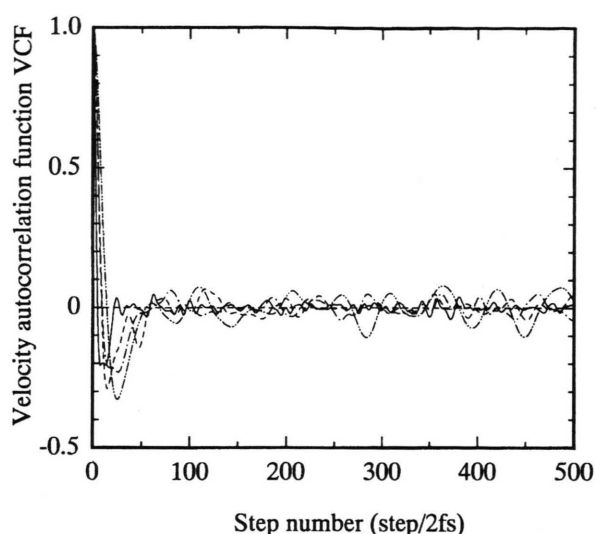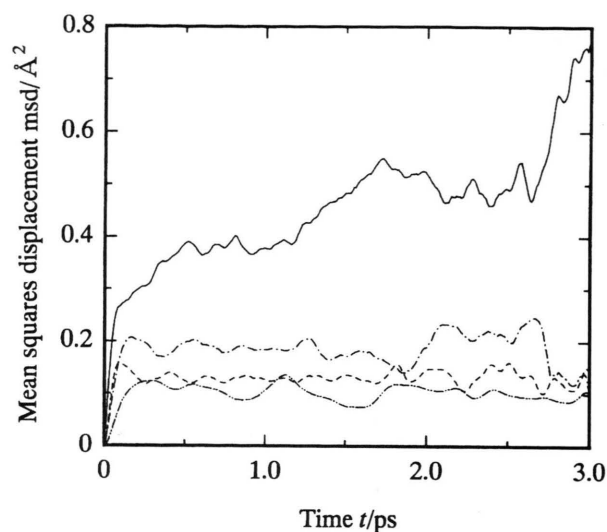
Fig. 2. Relationship between the mean squares displacements of exchangeable cations in sodalite framework and the time at 673 K. *Top: Monovalent cations.* Li: solid line, Na: broken line, K: chain line, Cs: double chain line. *Bottom: Multivalent cations.* Sr: solid line, Ba: broken line, La: chain line, Nd: double chain line.

Fig. 3. Relationship between the normalized velocity autocorrelation functions of exchangeable cations in sodalite framework and the step number at 673 K. *Top: Monovalent cations.* Li: solid line, Na: broken line, K: chain line, Cs: double chain line. *Bottom: Multivalent cations.* Sr: solid line, Ba: broken line, La: chain line, Nd: double chain line.

(b) Zeolite

During several picosecond the temperature controlled runs most Na ions have remained near the starting X-ray positions. The MD system used for the simulation in the Pm3m space group was a cubic box of 24.584 Å side. The MSD's for monovalent and multivalent cations are shown in Figure 4. The obtained self-diffusion coefficients from MSD's and

estimated adsorption selectivity in zeolite are as following orders

$$D_{Cs} < D_K < D_{Na} < D_{Li} \tag{4a}$$
$$\text{(monovalent cations in zeolite)}$$

$$D_{Sr} \approx D_{Nd} \approx D_{Ba} < D_{La} \tag{4b}$$
$$\text{(multivalent cations in zeolite)}$$

$$Li < Na < K < La < Cs < Ba < Nd < Sr \tag{4c}$$
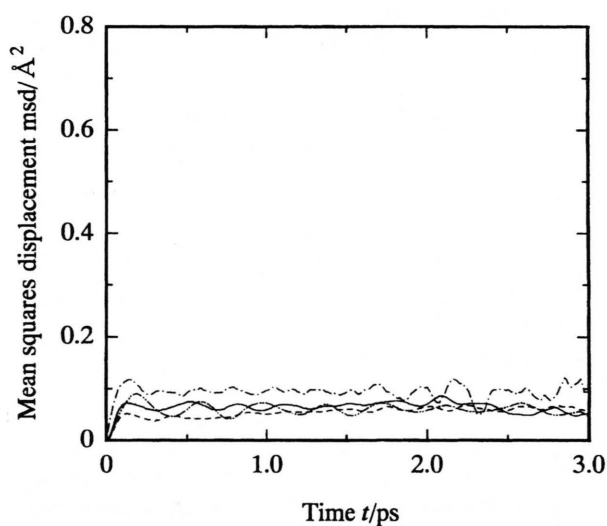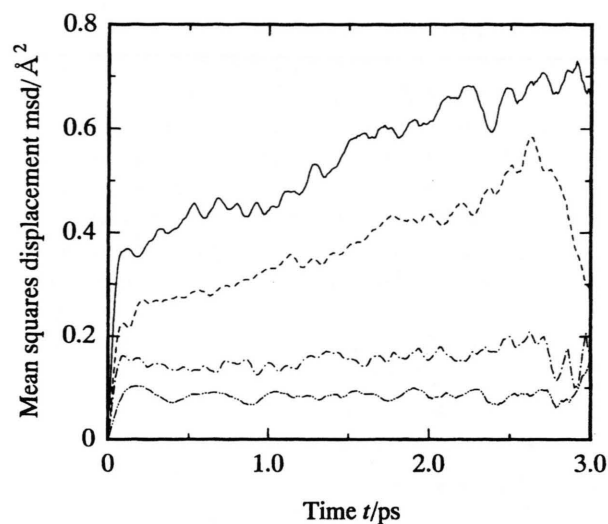$$\text{(adsorption selectivity in zeolite)}$$

Fig. 4. Relationship between the mean squares displacements of exchangeable cations in zeolite framework and the time at 673 K. *Top: Monovalent cations*. Li: solid line, Na: broken line, K: chain line, Cs: double chain line. *Bottom: Multivalent cations*. Sr: solid line, Ba: broken line, La: chain line, Nd: double chain line.
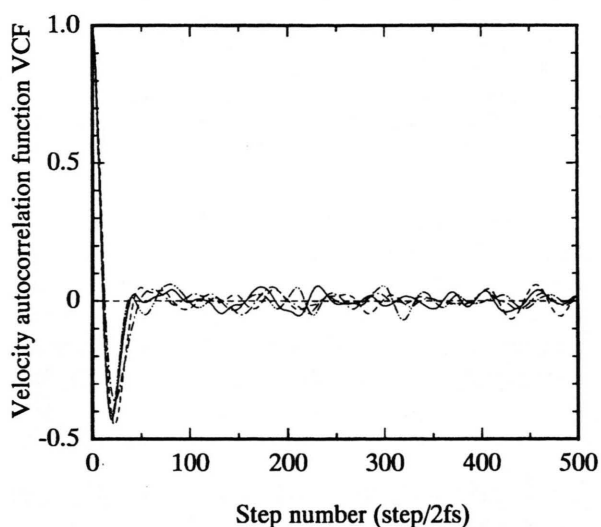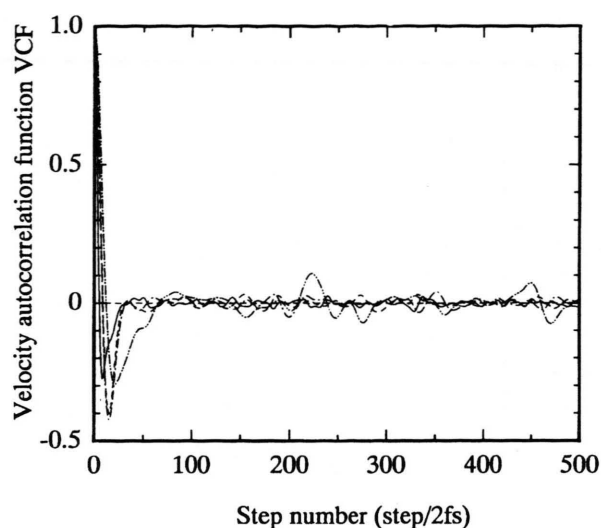
Fig. 5. Relationship between the normalized velocity autocorrelation functions of exchangeable cations in zeolite framework and the step number at 673 K. *Top: Monovalent cations*. Li: solid line, Na: broken line, K: chain line, Cs: double chain line. *Bottom: Multivalent cations*. Sr: solid line, Ba: broken line, La: chain line, Nd: double chain line.

The obtained self-diffusion coefficient of Na$^+$ agrees fairly with other reference data [39, 40] estimated by an other potential. The motion of Li ions is relatively more vigorous than that of the other ions, due to the small ionic radius. This is consistent with experimental observations [41] on the adsorption selectivity on zeolite. The self-diffusion coefficients of multivalent cations are smaller than those of monovalent cations. Thus, the multivalent ions are preferentially recov-

ered within the zeolite frameworks. The Cs ion, due to its large ionic radius, remains which would be close to the cavity of the α-cage in zeolite.

The VCF's of monovalent and multivalent exchangeable cations are shown in Figure 5. The VCF of the Na ions, very rapidly changing to negative values and then to positive ones, indicates that these ions are bouncing to the nearest framework atoms, back and forth, in the closed cages of the 8-ring windows.
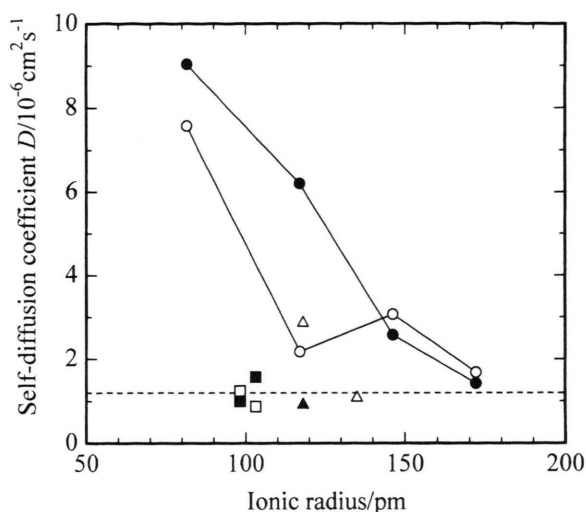
Fig. 6. Relationship between the self-diffusion coefficient of exchangeable cations in sodalite and zeolite frameworks and the ionic radius of monovalent cations in sodalite; white circles: monovalent cations in zeolite; black circles: divalent cations in sodalite; white triangles: divalent cations in zeolite; black triangles: trivalent cations in sodalite; white squares: trivalent cations in zeolite; black squares: trivalent cations in sodalite.

This vibrational character of diffusion can be seen in their MSD in Figure 4. In addition, the mobility of the each monovalent ion is completely different, because the depth and position of the first peak in VCF are divergent for each monovalent ions. The VCF decreases very rapidly at the initial, which means that mono-valent ions are not kept at their sites and easily diffuse away. On the other hand, the position and depth of the VCF's of multivalent ions are almost equal.

Relationship between the self-diffusion coefficients of exchangeable cations in sodalite and zeolite frameworks, and their ionic radius is indicated in Figure 6. It shows that the adsorption selectivity of multivalent cations is similar and independent of the ionic radius. Then, the self-diffusion coefficient of the monovalent cations is decreasing with increasing the ionic radius, and the adsorption selectivity of monovalent cations is consistent with the experimental results [41].

4. Conclusion

We have investigated the self-diffusion coefficients of exchangeable cations in aluminosilicates and the adsorption selectivity at 673 K by MD simulation. The self-diffusion coefficients of the monovalent cations are decreasing with increasing the ionic radii, and the orders of the self-diffusion coefficients calculated from the MD simulations are consistent with the experimental results. We found that the multivalent cations are more stable in aluminosilicates than the monovalent cations. These results allow to conclude that it is effective to recover alkali metals, in particular Cs, in aluminosilicates framework after the multivalent cations have been removed from the melt bath.

[1] M. Matsumiya and R. Takagi, Z. Naturforsch., to be submitted.

[2] M. Matsumiya, H. Matsuura, R. Takagi, and R. Fujita, J. Alloys Compd. **306**, 87 (2000).

[3] M. Matsumiya, R. Takagi, and R. Fujita, J. Nucl. Sci. Technol. **34**, 310 (1997).

[4] M. Matsumiya and R. Takagi, Z. Naturforsch. **55a**, 673 (2000).

[5] M. Matsumiya, M. Takano, R. Takagi, and R. Fujita, J. Nucl. Sci. Technol. **35**, 836 (1998).

[6] M. Matsumiya, M. Takano, R. Takagi, and R. Fujita, Z. Naturforsch. **54a**, 739 (1999).

[7] M. Matsumiya, R. Takagi, and R. Fujita, J. Nucl. Sci. Technol. **35**, 137 (1998).

[8] Y. I. Chang et al., ANL-IFR-246 (1994).

[9] M. Matsumiya, H. Matsuura, R. Takagi, and R. Fujita, J. Electrochem. Soc. **147**, 11 (2000).

[10] M. Matsumiya and R. Takagi, Z. Naturforsch. **55a**, 856 (2000).

[11] M. Matsumiya and R. Takagi, Z. Naturforsch. **56a**, 279 (2001).

[12] M. Iwasaki, and R. Takagi, J. Nucl. Sci. Technol. **31** [7] 751 (1994).

[13] R. Ohashi, M. Matsumiya, H. Matsuura, and R. Takagi, Electrochemistry **67**, 550 (1999).

[14] H. Matsuura, I. Okada, R. Takagi, and Y. Iwadate, Z. Naturforsch. **53a**, 45 (1998).

[15] M. Matsumiya and R. Takagi, Z. Naturforsch, to be submitted.

[16] M. Kubota, I. Yamaguchi, H. Nakamura, K. Okada, F. Mizuno, and T. Sato, JAERI-M 82-144 (1982) [in Japanese].

[17] R. Mori, I. Yamaguchi, and K. Kawamura, JAERI-M 86-013 (1986) [in Japanese].

[18] H. Mimura, K. Akiba, and K. Kawamura, J. Nucl. Sci. Technol., **31**, 463 (1994).

[19] Y. I. Chang, L. C. Walters, J. E. Battles, D. R. Pedersen, D. C. Wade, and M. J. Lineberry, ANL-IFR-125 (1990).

[20] P. Demontis, G. B. Suffritti, A. Alberti, S. Quartieru, E. S. Fois, and A. Gamba, Gazz. Chim. Ital. **116**, 459 (1986).

[21] P. Demontis, G. B. Suffritti, S. Quartieri, E. S. Fois, and A. Gamba, "Dynamics of Molecular Crystals" ed. By J. Lascombe, Elsevier, Amsterdam 1987, p. 699.

[22] P. Demontis, G. B. Suffritti, S. Quartieri, E. S. Fois, and A. Gamba, Zeolites **7**, 522 (1987).

[23] P. Demontis, G. B. Suffritti, S. Quartieri, E. S. Fois, and A. Gamba, J. Phys. Chem. **92**, 867 (1988).

[24] P. Demontis, E. S. Fois, G. B. Suffritti, and S. Quartieri, J. Phys. Chem. **94**, 4329 (1990).

[25] P. Demontis, G. B. Suffritti, S. Quartieri, A. Gamba, and E. S. Fois, J. Chem. Soc. Faraday Trans., **87**, 1657 (1991).

[26] E. Cohen de Lara, R. Kahn, and A. M. Goulary, J. Chem. Phys. **90**, 7482 (1989).

[27] E. Cohen de Lara and R. Kahn, J. Phys. **42**, 1029 (1981).

[28] J. M. Shin, K. T. No, and M. S. Jhon, J. Phys. Chem. **92**, 4533 (1988).

[29] LONS AND SCHULZ, 1967.

[30] L. Leherte, G. C. Lie, K. N. Swamy, E. Clementi, E. G. Derouane, and J. M. Andre, Chem. Phys. Lett. **145**, 237 (1988).

[31] L. Leherte, J. M. Andre, D. P. Vercauteren, and E. G. Derouane, J. Molec. Catal. **54**, 426 (1989).

[32] L. Leherte, J. M. Andre, E. G. Derouane, and D. P. Vercauteren, J. Chem. Soc., Faraday Trans. **87**, 1959 (1991).

[33] L. Leherte, J. M. Andre, E. G. Derouane, and D. P. Vercauteren, Computers Chem. **15**, 273 (1991).

[34] P. P. Ewald, Ann. Phys. **64**, 253 (1921).

[35] L. V. Woodcock, Chem. Phys. Lett. **10**, 257 (1971).

[36] J. J. Pluth and J. V. Smith, J. Amer. Chem. Soc. **102**, 4704 (1980).

[37] S. Beran and J. Dubsky, J. Phys. Chem. **83**, 2538 (1979).

[38] N. Wax, Selected Papers on Noise and Stochastic Processes, Dover 1954.

[39] G. K. Moon, S. G. Choi, H. S. Kim, and S. H. Lee, Bull. Korean Chem. Soc. **13** (3), 317 (1992).

[40] J. M. Shin, K. T. No, and M. S. Jhon, J. Phys. Chem. **92**, 4533 (1988).

[41] M. A. Lewis et al., J. Amer. Ceram. Soc. **76** [11], 2826 (1993).